



# Fractional Order PD(1+ PI) Controller for Frequency Control of Power System with Renewable Sources and Electric Vehicle

Asini Kumar Baliarsingh<sup>1</sup>, Sangram Keshori Mohapatra<sup>1</sup>, Pabitra Mohan Dash<sup>2</sup>

<sup>1</sup>Department of Electrical Engineering, Government College of Engineering, Odisha, India

<sup>2</sup>Department of Electrical Engineering, BEC, Odisha, India

**Cite this article as:** A. Kumar Baliarsingh, S. "Keshori Mohapatra and P. Mohan Dash, Fractional order PD(1+ PI) controller for frequency control of power system with renewable sources and electric vehicle," *Electrica*, 24(2), 406-424, 2024.

## ABSTRACT

This article introduces hybrid Arithmetic Optimization Algorithm (AOA) and Local Unimodal Sampling (hAOA-LUS)-based fractional order (FO) proportional derivative (PD) cascaded with one plus proportional integral (1+PI) controller for automatic generation control of power system with renewable energy sources (RES) and electric vehicle (EV). The control-area 1 has thermal, hydro, gas, and wind power generators and the same true for control area 2, which uses thermal, hydro, gas, and solar energy sources. Initially, Proportional-Integral-Derivative (PID) controllers are taken into consideration and it has been demonstrated that hAOA-LUS outperforms as compared to the AOA, Particle Swarm Optimization, and Generic Algorithm (GA). The assessing of overshoots, undershoots, and different integral errors of frequency and tie-line power deviations after step load perturbations in each area allows for performance comparison of the proposed power system. In the next stage, EVs are considered in each area and the controller parameters are optimized by hAOA-LUS techniques in the presence of RES and EV. A comparative analysis is carried out by hAOA-LUS-tuned FO PD(1+PI) controller with PID as well integer ordered PD(1+PI) for various cases so as to validate the superiority of the anticipated controller. The results from MATLAB and OPAL-RT are compared in order to verify the authenticate feasibility of method.

**Index Terms**—Arithmetic optimization algorithm, automatic generation control, fractional order (FO), local unimodal sampling, PD(1+ PI) controller

## Corresponding author:

Sangram Keshori Mohapatra

## E-mail:

sangram.muna.76@gmail.com

**Received:** September 16, 2023

**Revision Requested:** November 6, 2023

**Last Revision Received:** January 29, 2024

**Accepted:** March 2, 2024

**Publication Date:** May 14, 2024

**DOI:** 10.5152/electrica.2024.23143



Content of this journal is licensed under a Creative Commons Attribution-NonCommercial 4.0 International License.

## I. INTRODUCTION

The tie-line power and frequency in an interconnected power system diverge from their nominal values due to unsystematic changes in load. An automatic control system is required for maintaining frequency and generation in balance. By controlling the generations in the power system appropriately, the automatic generation control (AGC) method lowers the frequency and tie-line power variations [1].

### A. Literature Review

In the literature, various strategies for the AGC of power systems have been used. The main purpose of AGC is to reduce the area control error (ACE) and maintain the system frequency [2–3]. In the AGC system of diesel/wind turbine generators, numerous researchers have used a variety of secondary controllers, including conventional PID controllers [4]. A cascaded controller with a variety of groupings such as PI-PD [5], PD-PID [6], 2 degrees of freedom plus PID [7], a fuzzy logic-based PID controller [8], and fuzzy logic PI [9] have been anticipated in the literature. Traditional PID controllers are often preferred because of their user-friendly characteristics and ease of use in a variety of applications. The various PID enhancements have been anticipated in the literature to enhance the transient performances. Also, recently, fractional order (FO)-based controllers have gained popularity due to their improved performance over integer order configurations. The time domain analysis of FO concept  $PI^{\alpha}D^{\beta}$  controller involving FO integrator and FO differentiator is introduced [10]. It is provided for the necessity of such controllers for the more efficient control of FO system as compared to classical PID controller. The FO PID (FOPID) controller has been giving better performance and robustness and more suitable controller to address the challenges of the wind turbine system [11]. This controller gives less steady state error, less settling time, and robustness to noise and disturbances. The Integrated Power Systems of Electric Vehicles with Hybrid African Vulture Optimisation Algorithm and Pattern Search Tuned Fractional Order PID

Controller for AGC has been attempted for improvement of frequency regulation of the power system [12]. An optimal design of a robust FO-multistage controller for frequency control of an AC microgrid has been presented in the power system [13]. An improved Grey Wolf Optimization (GWO) design FO based type-2 fuzzy controller for microgrid frequency control has been presented in the system [14]. In the present study, a FO PD with a One Plus PI (1+PI) controller is anticipated for frequency control in the power system considered. The proposed FO-PD(1+PI) controller has the advantage of overcoming the disadvantage of simple controllers. It is anticipated that the system's performance will increase with these controllers because there are more control nodes. The disadvantages of this control structure are related to its increased complexity and the additional measurement device and controller.

In the current power system, mainly shares of electrical power are supplied by thermal and hydroelectric units, and a small portion is given by gas units. The renewable energy sources like solar and wind are now being combined to meet the demands of power. The consumers are moving to electric vehicles (EVs) due to the quick depletion of crude oil, severe greenhouse gas emissions that contribute to global warming, vibrant energy pricing policies, new pollution requirements, and steadily rising fuel prices. Electric vehicles have a battery replacing the petrol tank and an electric motor replacing an IC engine. They consume real power during charging and supply it during discharging. Batteries have an intrinsic feature of a quick reaction [15]; consequently, a group of EVs truly operates exceptionally efficaciously in stabilizing load and frequency variations [16] while working as a vast energy source.

Literature analysis demonstrates that many strategies are applied to construct controllers for AGC. A SGWO is provided in [17] and recommended for adaptive FPID structure designing of DPGS with energy storage using EV. It has been proposed a novel hybridized harmony search-random search algorithm designed fuzzy-3D controller structure used to control the frequency of an integrated hybrid power system with variable energy sources [18]. A robust fractionally ordered 3DOF-FOPID based control structure used for management of active power in a wind/solar hybrid power system has been suggested in the hybrid power system [19]. Studies have been conducted on the relative effectiveness of hybrid differential evolution and pattern search technique for electric power system frequency regulation [20]. The frequency management of electric power systems for the designing and analysis of the 2DOF-PIDN-FOID controller are described [21]. The various techniques, such as the Grasshopper Optimization Algorithm (GOA) [22], Sunflower Optimization [23], and the Sine Cosine Algorithm (SCA) [24], Symbiotic Organism Search and Particle Swarm Optimization (PSO) [25], Equilibrium Optimization Algorithm [26], Whale optimization algorithm [27], GWO [28-29], etc. According to the "No Free Lunch Theorem", there is no technique available for all sorts of issues. So new techniques are always welcome to solve optimization problems.

## B. Research Gap and Motivation

Recently, Abualigah et al. projected an arithmetic-based technique known as the Arithmetic Optimization Algorithm (AOA) [30]. It is apparent from [30] that the AOA technique provides better outcomes compared to GA, PSO, Moth-Flame Optimization, Gravitational Search Algorithm, DE, GWO, Biogeography-Based Optimization, Flower Pollination Algorithm, Bat Algorithm, Firefly Algorithm, and

Cuckoo Search Algorithm. Being a global search method, AOA tends to get stuck in local optima. Local optimization techniques like the Local Unimodal Sampling (LUS) [31] algorithm are intended to search local areas. There is motivation for combining AOA and LUS because of their complementary strengths. Taking into account the aforementioned criteria, this article proposes a hybrid AOA and LUS (hAOA-LUS)-based FO PD cascaded with One plus PI (FO PD(1+PI)) controller for an AGC of a power system with solar, wind sources, and EV. A relative investigation is performed by the hAOA-LUS tuned FO PD(1+PI) controller with PID as well as integer-ordered PD(1+PI) for various cases so as to validate the advantage of the projected controller.

## C. Contribution

The novel contributions of the proposed analysis are described as below:

- To propose a hybrid AOA and LUS (hAOA-LUS) technique to design a FO PD(1+PI) controller for frequency control of a two-area multi-source power system in the presence of RES and EVs.
- To validate the supremacy of the proposed hybrid AOA-LUS with PID controller compared to other conformist techniques such as AOA, PSO, and GA of the same power system.
- The proposed hAOA-LUS based optimization technique is tuned with fractional order (FO) PD(1+PI) controller parameters of frequency control of the power system with EV is compared with the performances with the same technique tuned with PID, PD(1+PI), and FO PD(1+PI) controllers of the same power system but in the absence of EV.
- To demonstrate the superiority of the proposed frequency control approach in retaining system stability in the context of various disturbances subjected to adjusting for parameter variations and increasing or decreasing load in one or more areas.
- The Performance Index Assessment of hAOA-LUS optimized of different controllers PID, PD(1+PI), FO PD(1+PI), and FO PD(1+PI) with EV are compared. The overshoots, undershoots, and different integral errors with different SLP of the same power system.
- The suggested method is validated by comparing the MATLAB and OPAL results.

The paper is organized as follows: Section II describes the system under study, Section III analyzes the design of the controller and objective function, Section IV discusses the overview of the hybrid arithmetic optimization algorithm and local unimodal sampling method, Section V analyzes the results and discussions, and Section VI briefly presents the conclusion.

## II. SYSTEM UNDER STUDY

It is the system that is being demonstrated is shown in Fig. 1. In area 1, thermal, hydro, gas, and wind energy sources are taken into consideration. In area 2, thermal, hydro, gas, and solar energy sources are taken into consideration, and in each area, EVs are connected. The model of wind and solar sources is taken from [32], and the gas generator unit is taken from [16].

### A. Modeling of Components

#### 1) Thermal Power Plant

The various components of the thermal unit include a generator, governor, turbine, and reheater. Their transfer function representation is [3].

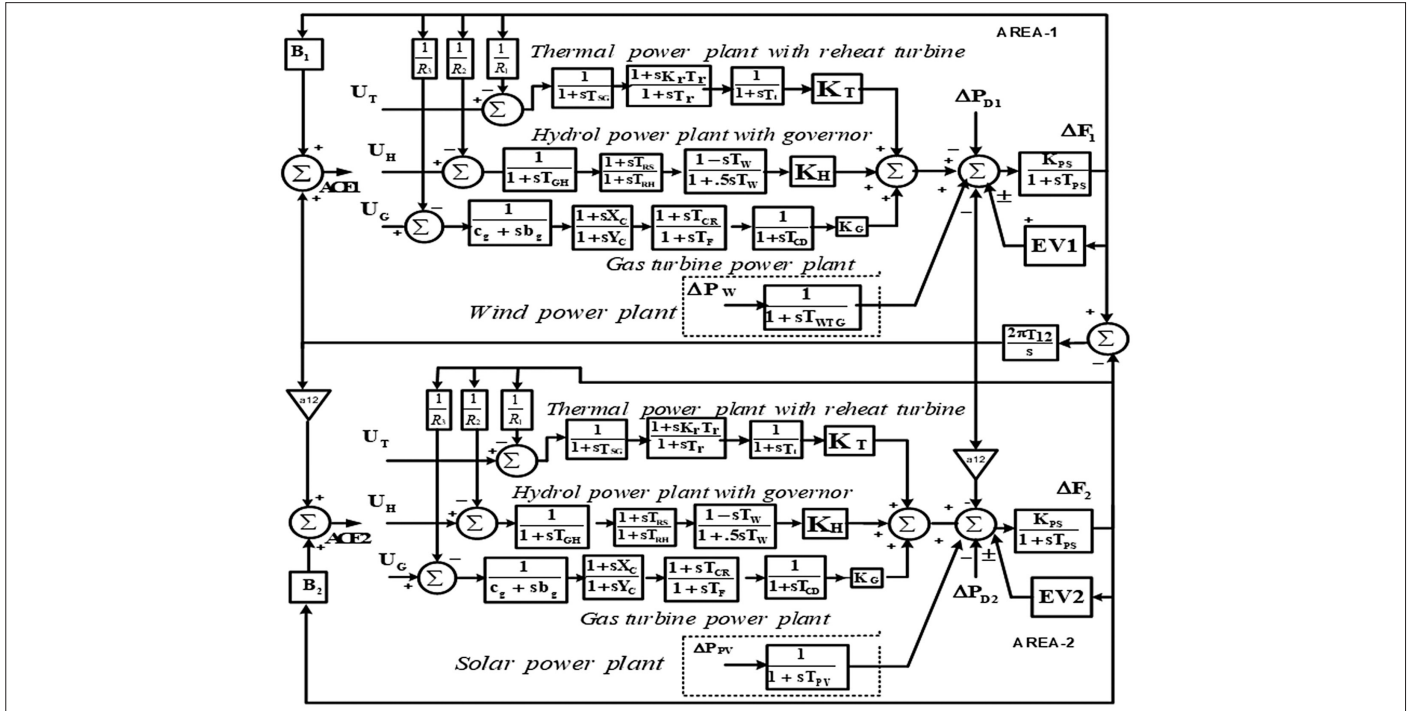


Fig. 1. System under study in two areas with multi sources.

$$G_p(s) = \frac{K_p}{1+sT_p} \quad (1)$$

$$G_g(s) = \frac{K_g}{1+sT_g} \quad (2)$$

$$G_t(s) = \frac{K_t}{1+sT_t} \quad (3)$$

$$G_r(s) = \frac{1+sK_rT_r}{1+sT_r} \quad (4)$$

### 2) Hydro Power Plant

The transfer function of "hydraulic governor" and "turbine" is [33]:

$$G_{HG}(s) = \left[ \frac{K_1}{1+sT_1} \right] \left[ \frac{1+sT_R}{1+sT_2} \right] \quad (5)$$

$$G_r(s) = \frac{1+sT_W}{1+0.5*sT_w} \quad (6)$$

where  $T_1, T_2, T_{R1}, T_2,$  and  $T_w$  represents the "hydro plant's speed governor," "main servo time constant," "reset time," "starting time of water in penstock," respectively.

### 3) Gas Power Plant

A gas unit includes a valve positioner, speed governor system, fuel system, combustor, and gas turbine, as illustrated in Fig. 1, where  $c_g$  is the gas turbine valve positioner and  $b_g$  is the gas turbine constant

of the valve positioner.  $X_C$  and  $Y_c$  are the lead and lag time constants of the governor in sec, Time constant for turbine fuel represented as  $T_f$  and time delay for turbine combustion is represented as  $T_{CR}$  discharge volume-time constant ( $T_{CD}$ ) [16].

### 4) Wind Turbine Generator

The wind turbine is illustrated by power coefficient  $C_p$  as an element of both the tip speed proportion  $\lambda$  and blade pitch point  $\beta$ . The  $\lambda$  is given by [32]:

$$\lambda = \frac{R_{blade}\omega_{blade}}{V_w} \quad (7)$$

where  $R_{blade}$  represents the radius blades and  $\omega_{blade}$  shows the speed of blades.

The  $C_p$  is computed as:

$$C_p = (0.44 - 0.0167\beta) \sin \left[ \frac{\Pi(\lambda - 3)}{15 - 0.3\beta} \right] - 0.0184(\lambda - 3)\beta \quad (8)$$

The expression for the output power of the wind turbine is:

$$P_{WP} = \frac{1}{2} \rho A_R C_p V_w^3$$

where  $\rho$  displays the air density and  $A$ , is the swept area of blades. For low low-frequency studies, it is denoted as [30]:

$$G_{WTG}(s) = \frac{K_{WTG}}{1+ST_{WTG}} \quad (9)$$

### 5) Solar PV

The PV power output is specified by [1]:

$$P_{pv} = \eta S \gamma [1 - 0.005 (T + 25)], \quad (10)$$

Where,  $\eta$  = PV cell conversion efficiency with a value of 10%,  $S$  = PV array area with a value of 4084m<sup>2</sup>

$\phi$  = solar irradiation in kW/m<sup>2</sup>,  $T_a$  = ambient temperature in degree Celsius ( $T = 25^\circ\text{C}$ ).

When analyzing this system in the low-frequency domain, the first order transfer function is represented by:

$$G_{PV}(s) = \frac{K_{PV}}{1 + sT_{PV}} = \frac{\Delta P_{PV}}{\Delta \phi} \quad (11)$$

### 6) EV Modeling

It is expected that electric cars (EVs) would be widely utilized in future power networks due to the increased demand for EVs. The opportunity to use batteries while plugging in is provided by EVs. If an EV fleet were to exist, it might serve as an auxiliary facility for the future power system. Thus, it is essential to assess EVs' capacity for frequency control over the system under study. The two-area interconnected power system with EV is taken as the test system. Electric vehicles are used in hybrid power systems for improving stability against fluctuations in load demands. Fig. 2 shows the transfer function model of EV. The figure presents the modeling of EV for frequency control and is also demonstrated in Fig. 2 [28]. The LFC signal  $\Delta U$  is supplied to EV for discharging/charging. The parameters  $\pm B_{kw}$  signify the battery capacity. The existing battery energy is signified by  $E$  that is kept within the restrictions  $E_{\max}$  and  $E_{\min}$  presumed as 90% and 80%.  $K_1$  and  $K_2$  are found as  $K_1 = E - E_{\max}$ ,  $K_2 = E - E_{\min}$ . The stored energy part in Fig. 2 computes the remaining stored energy. When the charge reaches the limitation levels, there is no involvement of EV's in AGC. The net battery stored energy is estimated by the stored energy subsystem in a local control center that operates as a connection between the power grid and EVs [17].

## III. CONTROLLER STRUCTURE AND OBJECTIVE FUNCTION

### A. Controller Structure

It has been shown that an FO controller improves the performance of a PID controller [30]. In view of the above FO-based PD(1+PI) controllers, they are proposed here for AGC. Fig. 3 shows the assembly of FO PD(1+PI). The total transfer function of the FO PD(1+PI) controller is provided by:

$$TF_{FO PD-(1+PI)} = (K_{P_1} K_D s^\lambda) (1 + K_{PP_1} K_I / s^\mu) \quad (12)$$

In the FO PD(1+PI) control model Fig. 3,  $K_{P_1}$ ,  $K_I$ ,  $K_D$ ,  $K_{PP_1}$  are PID gains, the second-stage P-gain and  $\lambda$  and  $\mu$  are the order of derivative and integrator. Area control error is accepted as an input signal, and the output is used as the reference power setting of different equipment. For a fractional operator, the frequency range is taken from 0.001 to 1000, and the approximation order is taken as 5. The ACE is measured by linearly evaluating the system frequency and tie-line power errors, which are represented as follows:

$$ACE_i = \beta_i \Delta F_i + \sum_{j=1}^n \Delta P_{ij} \quad (13)$$

### B. Objective Function

To achieve the required action, the appropriate choice of the objective function ( $J$ ) is essential. An integral square error (ISE) which tends to decrease the frequency variations ( $\Delta F_i$ ) and tie-line power variations ( $\Delta P_{tie-i-j}$ ) and control action ( $\Delta U$ ) is introduced as  $J$  as:

$$J = \int_0^t [k_n w ((\Delta F_i)^2 + (\Delta P_{tie-i-j})^2) + (1-w)(\Delta U)^2] dt \quad (14)$$

Where  $t$  is time. To guarantee the both components in Eq. (14) participate in the optimization,  $k_n$  and  $w$  are allotted values of 200 and 0.5, respectively. The  $J$  is minimized to selecting the controller parameters subject to the constraints given by  $K_{P_{Min}} \leq K_P \leq K_{P_{Max}}$ ,  $K_{D_{Min}} \leq K_D \leq K_{D_{Max}}$ ,  $K_{I_{Min}} \leq K_I \leq K_{I_{Max}}$ ,  $K_{PP_{Min}} \leq K_{PP} \leq K_{PP_{Max}}$ ,  $\lambda_{Min} \leq \lambda \leq \lambda_{Max}$ ,  $\mu_{Min} \leq \mu \leq \mu_{Max}$ . The subscripts Max and Min signify the minimum and maximum values of corresponding parameters. To evaluate the system performance various integral based  $J_s$  like IAE, ISE, ITAE, ITSE, and ISTAE are used as given below:

$$J_1 = ISE = \int_0^t ((\Delta F_i)^2 + (\Delta P_{tie-i-j})^2) dt \quad (15)$$

$$J_2 = ITSE = \int_0^t ((\Delta F_i)^2 + (\Delta P_{tie-i-j})^2) t dt \quad (16)$$

$$J_3 = IAE = \int_0^t (|\Delta F_i| + |\Delta P_{tie-i-j}|) dt \quad (17)$$

$$J_4 = ITAE = \int_0^t (|\Delta F_i| + |\Delta P_{tie-i-j}|) t dt \quad (18)$$

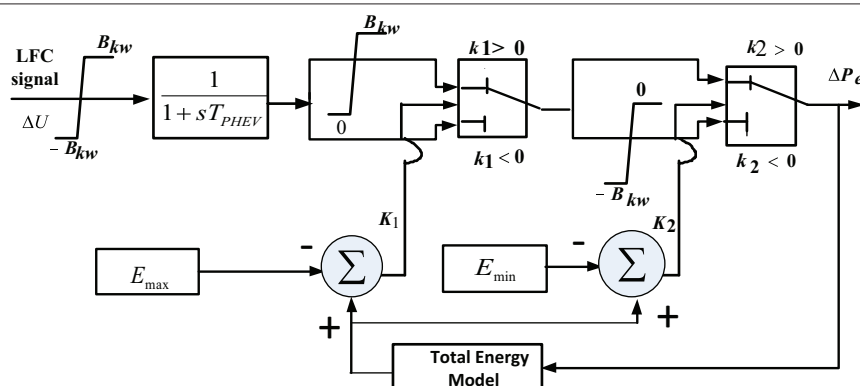
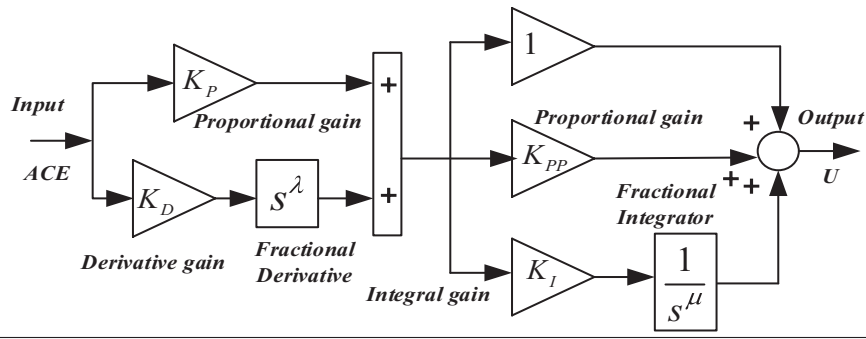


Fig. 2. Transfer function model two area with EV.



**Fig. 3.** Controller design of FO-PD-(1+PI) controller

$$J_s = ISTAE = \int_0^t (|\Delta F_i| + |\Delta P_{tie\ i-j}|) t^2 dt \quad (19)$$

where  $\Delta F_i$  = frequency deviation in the  $i^{th}$  area,  $\Delta P_{tie\ i-j}$  = tie-line power change between  $i^{th}$  and  $j^{th}$  areas.

#### IV. HYBRID ARITHMETIC OPTIMIZATION ALGORITHM AND LOCAL UNIMODAL SAMPLING METHOD

##### A. Arithmetic Optimization Algorithm

Recently, Abualigah *et al.* proposed an arithmetic-inspired technique known as AOA [28]. The foundation of AOA is the generation of a group of solutions to any optimization problem that are then enhanced by an optimization rule that has been adopted. By finding new solution search spaces and updating accuracy based on the best solutions found, the 2 mechanisms in this process—exploration and exploitation—ensure that the best solution has been identified. These stages of AOA are accomplished with the use of mathematical arithmetic operators, including Division (D, “÷”), Addition (A, “+”), Subtraction (S, “-”), and Multiplication (M, “×”). It is initialized randomly across the search space (s) in the candidate solutions of size Z, which is represented by a matrix  $P_{(Z \times s)}$ , which is provided by

$$P_{(Z \times s)} = \begin{bmatrix} p_{1,1} & \dots & p_{1,j} & \dots & p_{1,n} \\ \vdots & \dots & \vdots & \dots & \vdots \\ p_{i,1} & \dots & p_{i,j} & \dots & p_{i,n} \\ \vdots & \dots & \vdots & \dots & \vdots \\ p_{z,1} & \dots & p_{z,j} & \dots & p_{z,s} \end{bmatrix} \quad (20)$$

Then, the search phase is decided by a coefficient Math Optimizer Accelerated (MOA), and is calculated as

$$MOA(C\_it) = A_{min} + C\_it \times \left( \frac{A_{max} - A_{min}}{M\_it} \right) \quad (21)$$

Where  $C\_it$  and  $M\_it$  signify the present and maximum iterations,  $A_{min}$  and  $A_{max}$  are the range of the accelerated function. Then, the  $j^{th}$  position of  $i^{th}$  solution has updating the exploration phase by employing the division and multiplication operators which is given by

$$p_{i,j}(C\_it+1) = \begin{cases} best(p_j) \div (MOP + \delta) \times ((U_{bj} - L_{bj}) \times \mu + L_{bj}), & rnd_1 < 0.5 \\ best(p_j) \times (MOP) \times ((U_{bj} - L_{bj}) \times \mu + L_{bj}), & otherwise \end{cases} \quad (22)$$

where coefficient  $MOP$  is known as Math Optimizer Probability and is obtained as

$$MOP(C\_it) = 1 - \frac{C\_it^{(\alpha)}}{M\_it^{(\alpha)}} \quad (23)$$

where  $\alpha$  and  $\mu$  represent the sensitive and control parameters, respectively.  $best(p_j)$  signifies the global solution attained in  $j^{th}$  positions.  $U_{bj}$  and  $L_{bj}$  are the bounds of the  $j^{th}$  position.  $\delta$  and  $rnd_1$  signify the small integer and an arbitrary number, respectively.

Then, during the exploitation phase, both addition and subtraction operators are used to update the  $j^{th}$  position of  $i^{th}$  solution which is given by

$$p_{i,j}(it+1) = \begin{cases} best(p_j) - (MOP) \times ((U_{bj} - L_{bj}) \times \mu + L_{bj}), & rnd_2 < 0.5 \\ best(p_j) + (MOP) \times ((U_{bj} - L_{bj}) \times \mu + L_{bj}), & otherwise \end{cases} \quad (24)$$

where  $rnd_2$  is a random number.

The detailed procedure of the AOA algorithm is as follows:

1. Initialize parameters  $\mu$  and  $\theta$  of the algorithm, Take  $t=0$
2. Initialize the n number of solutions positions randomly
3. **While** (stopping condition does not meet) do
4. Assess the fitness values of the generated solutions
5. Save the best solution achieved so far
6. Eq (21) is used to modify the MOA value
7. Eq (23) is used to modify the MOP value
8. **for** ( $i=1$  to solutions) do
9. **for** ( $j=1$  to Positions) do
10. Generate a random value (rand 1, rand2, and rand3) between [0,1]
11. **if** (rand1>MOA)
12. **//Exploration Stage**
13. **if** (rand2> 0.5)
14. Employ the division operator (D “÷”)
15. Using the first rule of Eq. (22), update the  $i^{th}$  solution’s position.
16. **else**
17. Employ the multiplication operator (M “×”)
18. Using the second rule of Eq. (22), update the  $i^{th}$  solution’s position.s

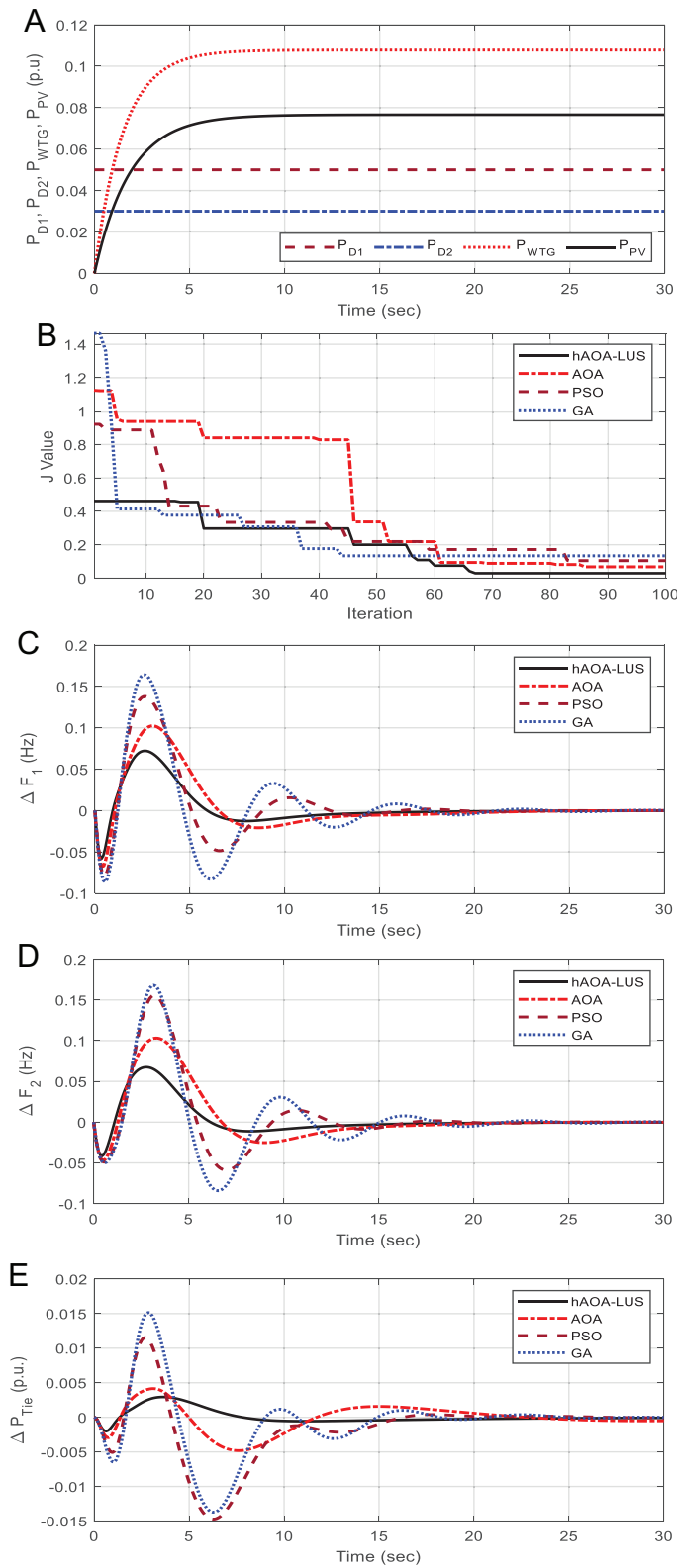


**Fig. 4.** (A–E) System responses comparison of optimization techniques with PID controller. (A)  $P_{D1}$ ,  $P_{D2}$ ,  $P_{WTG}$ ,  $P_{PV}$ , (B) Comparison of Convergence graphs of compared methods, (C)  $\Delta F_1$ , (D)  $\Delta F_2$ , (E)  $\Delta P_{Tie}$ .

**TABLE I.** G, PSO, AOA, AND HAOA-LUS TUNING PID-BASED CONTROLLER PARAMETERS OF THE SYSTEM

Unit/Parameters	Area 1			Area 2			Objective Function J Value $\times 10^{-1}$	
	Thermal Ppower Plant	Hydro Power Plant	Gas Power Plant	Thermal Power Plant	Hydro Power Plant	Gas Power Plant		
GA	$K_p$	-0.9452	-1.5366	1.6745	1.9782	0.683	-1.8475	1.33609
	$K_i$	1.8121	1.7315	0.7881	0.9123	-0.5126	1.2421	
	$K_D$	1.4583	1.7945	-1.6735	1.7316	1.6367	-1.0451	
PSO	$K_p$	-0.4895	-1.5674	1.7359	1.5792	0.4273	-1.7236	1.04752
	$K_i$	1.9828	1.8603	0.5533	0.5412	-0.3846	1.0343	
	$K_D$	1.3414	1.3933	-1.0081	1.6911	1.6909	-0.6119	
AOA	$K_p$	1.1167	0.3721	0.4943	1.3387	0.1472	0.1027	0.67815
	$K_i$	0.6723	1.4673	1.6398	1.4622	-0.4845	-0.6549	
	$K_D$	1.3267	1.4298	1.3578	1.2151	1.2568	0.6221	
hAOA-LUS	$K_p$	1.9181	1.5705	1.7711	1.8686	0.5154	1.4761	0.29324
	$K_i$	1.3526	1.4518	1.4455	1.9832	-0.3165	1.1353	
	$K_D$	1.9797	1.4195	1.8991	1.3765	1.2195	1.4175	

AOA, Arithmetic Optimization Algorithm; hAOA-LUS, hybrid Arithmetic Optimization Algorithm and Local Unimodal Sampling; PSA, particle swarm optimization.

```

19. end if
20. else
21. //Exploitation stage
22. if (r3>0.5)
23. Employ the Subtraction operator (S"-")
24. Using the first rule of Eq. (24), update the ith solution's position.s
25. else
26. Employ the addition operator (A "+")
27. Using the second of Eq. (24), update the ith solution's position.s
28. endif
29. end if
30. end for
31. end for
32. t=t+1
33. end While
34. Return the global best solution
    
```

### B. Local Unimodal Sampling

Some local search techniques like using a fixed sampling rate throughout the optimization are trapped in local optima. The sampling range varies for optimization in the LUS algorithm [29]. In the LUS algorithm, sampling procedure is done by selecting an innovative potential location signified as  $\bar{Y}$  from the neighborhood of the present location and  $\bar{D}$  as the present sampling range from the whole search area. Concurrently, the sampling for all dimensions is reduced when a sample is unable to progress. After a failure, the sampling choice is decreased to half and  $\bar{D}$  is multiplied by a parameter "Q" in each debacle.

The starting position  $\bar{X} \in \mathbb{R}^n$  is arbitrarily chosen for "n" dimensional problems. The modified location  $\bar{Y}$  is formed in the vicinity of  $\bar{X}$ .  $(-\bar{D}, +\bar{D})$  is engaged as the starting range, where  $\bar{D} = \bar{B}_{up} - \bar{B}_{low}$ .  $\bar{B}_{up}$  and  $\bar{B}_{low}$  are the boundaries of the search area.

**TABLE II.** PERFORMANCE INDEX COMPARISON OF VARIOUS METHODOLOGIES

Controller/Method	Integral Errors					Max. Overshoots (MO <sub>s</sub> )		Max. Undershoots (MU <sub>s</sub> ) (-ve)	
	ISE	ITAE	ITSE	IAE	ISTAE	$\Delta F_1$	$\Delta F_2$	$\Delta F_1$	$\Delta F_2$
GA	0.1268	8.7058	0.4830	1.5488	79.4827	0.1641	0.1681	0.0863	0.0842
PSO	0.0981	6.1060	0.3409	1.2645	46.0284	0.1380	0.1557	0.0788	0.0589
AOA	0.0602	6.0307	0.2201	1.0691	56.7096	0.1024	0.1032	0.0674	0.0469
hAOA-LUS	0.0249	3.1548	0.0745	0.6345	29.1302	0.0722	0.0674	0.0579	0.0416

AOA, Arithmetic Optimization Algorithm; hAOA-LUS, hybrid Arithmetic Optimization Algorithm and Local Unimodal Sampling; ISE, integral square error; PSA, particle swarm optimization.

So, the changed sampling rate is

$$\bar{D} = Q \times \bar{D} \quad (25)$$

Where  $Q = \sqrt[\gamma]{1/2}$ .

Usually, the value of  $\gamma=3$  is taken. If the fitness is better, the algorithm progresses from the old position  $\bar{X}$  to the new position  $\bar{Y}$ .

The steps of LUS are

1. Randomly initialize the current position  $\bar{X}$  in the search space.
2. Set the initial search range  $\bar{D}$  over the entire search space:  $\bar{D} \leftarrow \bar{B}_{up} - \bar{B}_{low}$
3. Repeat
  - i. Randomly select a vector  $\bar{A} \sim U(-\bar{D}, +\bar{D})$
  - ii. Position  $\bar{Y} = \bar{X} + \bar{A}$
  - iii. If the fitness at  $\bar{Y}$  is less than that at  $\bar{X}$ , upgrade  $\bar{X} \leftarrow \bar{Y}$
  - iv. Otherwise reduce the search range  $\bar{D}$  as  $\bar{D}_{new} = Q \times \bar{D}$
4. Until the fitness threshold is met.

The MATLAB code for local Unimodal Sampling utilized in this study has been programmed. With a sample range that initially encompasses the whole search universe and as the advances of optimization which are reduced exponentially and a LUS optimizer conducts localized sampling in the search space. When solving optimization issues where only brief runs are possible, the LUS performs

particularly well. The settings for local unimodal sampling are as follows: 30 suitable search agents, 100 iterations, and a random selection of the initial solution within the given bounds by MATLAB functions.

## V. RESULTS AND DISCUSSION

Investigations are performed to evaluate the effectiveness of the projected scheme for frequency regulation of the power system described in Fig. 1. The demonstration of the proposed system under different disturbances of 5% SLP in area 1 ( $P_{D1} = 0.05$ ), 3% SLP ( $P_{D2} = 0.03$ ) in area 2, wind power  $P_{WTG} = 0.1078$  p.u. ( $V_{wind} = 7.5$  m/s), and solar power of 0.07657 p.u. are taken for frequency control analysis of the system. The response of the change of power is shown in Fig. 4A. To authenticate the hAOA-LUS method, at first, PID controllers are considered and EVs are not considered. The controllers are tuned by AOA, PSO, and GA methods. The details of these methods are given in the appendix. The setting of controller parameters taken between the boundary of  $[-2, 2]$ . The initial parameters of optimization techniques GA, PSO, AOA, and hAOA-LUS search agents = 30 and iteration = 100 and ran 30 times are the same for all the techniques. The best values related to the minimum J achieved are regarded as the optimal parameters as collected in Table I. The convergence curve of each comparison method is illustrated in Fig. 4B. It is clear from the results that minimum value of the objective function J is achieved with AOA compared to GA and PSO. The objective function J value is further with hAOA-LUS. The

TABLE III. OPTIMAL CONTROLLER PARAMETERS BY HAOA-LUS TECHNIQUE

Unit/Parameters		Area 1			Area 2			Objective Function (J)
		Thermal Power Plant	Hydro Power Plant	Gas Power Plant	Thermal Power Plant	Hydro Power Plant	Gas Power Plant	
PD-(1+PI)	$K_p$	1.6243	1.1800	1.3054	1.6519	0.7778	1.1157	1.6341
	$K_i$	0.5455	0.93653	1.1775	0.9852	0.8874	0.5318	
	$K_D$	1.5329	1.1013	1.2552	1.1260	1.0128	1.1179	
	$K_{pp}$	1.1808	0.2249	1.0601	1.6784	1.2938	1.4265	
FO PD-(1+PI)	$K_p$	1.5659	1.6504	1.1586	1.5734	1.5418	1.2064	1.2831
	$K_i$	1.0769	1.7338	1.5861	1.5319	1.5756	1.0707	
	$K_D$	1.5695	1.1552	1.5802	1.0118	1.0637	1.3367	
	$K_{pp}$	1.0871	1.3749	1.8942	1.6418	1.8477	1.9103	
	$\lambda$	0.8476	0.9378	0.5955	0.7476	0.8990	0.6684	
	$\mu$	0.6984	0.5847	0.6834	0.9573	1.1455	0.8592	
FO PD-(1+PI) with EV	$K_p$	1.9263	1.7591	1.9667	1.9123	1.6366	1.9295	0.6308
	$K_i$	1.8135	1.8408	1.9444	1.8884	1.9003	1.8193	
	$K_D$	1.9789	1.5539	1.7185	1.9242	1.2230	1.7197	
	$K_{pp}$	1.8992	1.8191	1.9003	1.8630	1.8796	1.9797	
	$\lambda$	1.1859	1.0539	0.8528	1.1017	1.0835	0.9588	
	$\mu$	1.1853	1.1092	1.0960	1.0067	1.1556	1.1579	

EV, electric vehicle; PD-(1+PI), proportional derivative cascaded with one plus proportional integral controller.

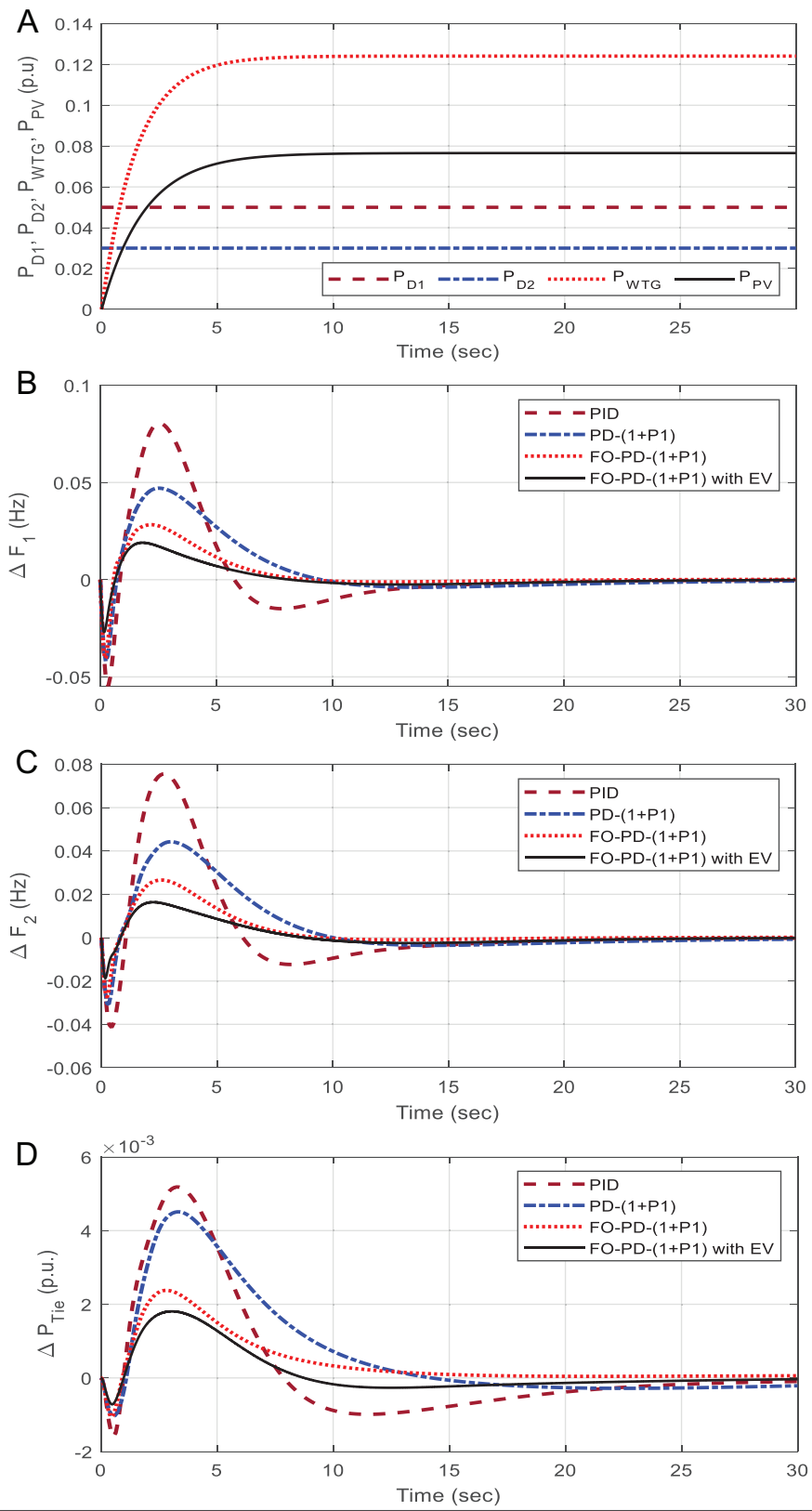


**Fig. 5.** (A–D) System responses of different disturbances, frequency deviation, and tie line power deviation for case 1. (A)  $P_{D1}$ ,  $P_{D2}$ ,  $P_{WTG}$ ,  $P_{PV}$ , (B)  $\Delta F_1$ , (C)  $\Delta F_2$ , (D)  $\Delta P_{Tie}$ .

**TABLE IV.** PERFORMANCE INDEX ASSESSMENT OF HAOA-LUS TUNING CONTROLLER PARAMETERS FOR CASE 1

Controller/Method	Objective Function (J)	Integral Errors					MO <sub>s</sub>		MU <sub>s</sub> (-ve)	
		ISE	ITAE	ITSE	IAE	ISTAE	ΔF <sub>1</sub>	ΔF <sub>2</sub>	ΔF <sub>1</sub>	ΔF <sub>2</sub>
PID	3.6504	0.0304	3.6250	0.0916	0.7135	34.1547	0.0805	0.0755	0.0546	0.0414
PD-(1+PI)	2.1396	0.0145	3.3552	0.0506	0.5507	40.1425	0.0471	0.0442	0.0419	0.0307
FO PD-(1+PI)	1.5580	0.0048	1.0705	0.0127	0.2660	8.1381	0.0283	0.0266	0.0404	0.0272
FO PD-(1+PI) with EV	0.8266	0.0020	1.4068	0.0063	0.2155	18.1811	0.0190	0.0164	0.0269	0.0187

EV, electric vehicle; FO, functional order; ISE, integral square error; PD-(1+PI), proportional derivative cascaded with one plus proportional integral controller.

% decrease in J value using the hAOA-LUS technique compared to GA, PSO, and AOA are 78.05%, 72.01%, and 56.75%, accordingly. The system dynamic responses for the aforesaid situation are depicted in Fig. 4c–e. It is seen from Fig. 4c–e that the hAOA-LUS approach in PID controller performance is superior to GA, PSO and AOA optimization algorithm. The evaluation description of transient performances employing multiple integral errors, maximum overshoots, and maximum undershoots of  $\Delta F_1$ ,  $\Delta F_2$ ,  $\Delta P_{Tie}$  of the anticipated system with PID controller improved by the above methodologies are presented in Table II. It is found that the numerical values of integral errors due to hAOA-LUS optimized PID controller are found to be the least compared same with GA, PSO, and AOA optimized PID controller. This demonstrates that the hAOA-LUS approach outperforms the GA, PSO, and AOA strategies in the investigated controller design problem.

In the next stage, hAOA-LUS technique is employed to optimize PD(1+PI) and FO PD(1+PI) controllers. The structure of PD-(1+PI) is similar to the FO PD(1+PI) shown in Fig. 3, but the FO derivatives and integrators are replaced by integer ordered derivatives and integrators. The optimized values are shown in Table III. It is clear that minimal J value is reached with FO PD(1+PI) compared to PD(1+PI). The J value is significantly decreased when EVs are considered. The % reduction in J value with FO PD(1+PI) with EV system compared to only FO PD(1+PI), PD(1+PI), and PID are 78.48%, 61.39%, and 50.83%, respectively. In order to compare the performances, a variety of cases (other than the ones for which the controllers are designed) are demonstrated in the system.

- Case 1: SLPs at each location without attention to disturbances from solar or wind sources
- Case 2: SLPs change with variation of wind speed but solar irradiance remains constant
- Case 3: SLP changes with variations in solar and wind sources
- Case 4: Uncertainty of system parameter
- Case 5: In the presence of nonlinearity

#### A. Case 1

In this case 1, the demonstration of the proposed system under disturbances of 5 percentage SLP in area 1 ( $P_{D1} = 0.05$ ), 3 percentage SLP ( $P_{D2} = 0.03$ ) in area 2, wind power  $P_{WTG} = 0.1241$  p.u. ( $V_{wind} = 9$  m/s) and solar power of 0.07657 p.u. are taken for the evaluation of frequency control analysis of the system. The changes of powers are shown in Fig. 5a. The system response with suggested hAOA-LUS optimized PID, PD(1+PI), FO PD(1+PI), and FO PD(1+PI) with EV are depicted in Fig. 5b–d. It can be seen from findings that the transient

stability improvement with FO PD(1+PI) with EV is greater than PID and PD(1+PI) controllers with minimum errors and maximum overshoots/undershoots relative to other controllers. The evaluation description of integral errors, MOs, and MUs of frequency deviation of area 1 ( $\Delta F_1$ ), frequency deviation of area 2 ( $\Delta F_2$ ), tie line power ( $\Delta P_{Tie}$ ) of the suggested system for the aforesaid scenario is presented in Table IV. It is found from results that the objective function J values, errors, maximum overshoots, and maximum undershoots due to FO PD(1+PI) with EV are found to be the least compared to other approaches. The percentage minimization of the objective function J value with FO PD(1+PI) compared to PID, PD(1+PI), and FO PD(1+PI) are 77.35%, 61.36%, and 46.94%, respectively, for Case 1.

#### B. Case 2

In case 2, SLPs of areas 1 and area 2 are raised by two percentage points, while wind speed ( $V_w$ ) is decreased by two meters per second at time  $t = 30$  seconds comparing to case 1. The variances of power are shown in Fig. 6a. The system response with hAOA-LUS tuned PID, PD(1+PI), FO PD(1+PI), and FO PD(1+PI) with EV are illustrated in Fig. 6b–d. It can be noticed that the transient stability improvement with FO PD(1+PI) with EV is better than PID, PD(1+PI), and FO PD(1+PI) controllers with respect to least errors and maximum overshoots/undershoots related to other controllers. The evaluation description is given in Table V from which it is observed that fewer values J, integral errors, maximum overshoots, and maximum undershoots due to FO PD(1+PI) with EV are found to be the least compared to other approaches. The % reduction of objective function J with proposed FO PD(1+PI) with EV compared to PID, PD(1+PI), and FO PD(1+PI) is 80.05%, 64.95%, and 53.87%, respectively, for Case 2.

#### C. Case 3

In this case 3, The disturbances of SLPs of areas 1 and area 2 are 1.5% lower, the wind speed is 3.5 m/s higher, and the solar radiation is 0.15 p.u. higher at time  $t = 60$  s for comparing to case 2 are considered for demonstration of frequency analysis of the system. These variation of load and power are represented as in Fig. 7a. The system response with anticipated hAOA-LUS optimized PID, PD(1+PI), FO PD(1+PI), and FO PD(1+PI) with EV are illustrated in Fig. 7b–d. It can be seen from Fig. 7b–d that, the transient stability improvement with FO PD(1+PI) with EV is better than PID, PD-(1+PI), and FO PD-(1+PI) controllers correlated to other controllers. The evaluation description for case 3 is given in Table VI. It is observed that better results are attained with FO PD(1+PI) with EV compared to other approaches. The % reduction of objective function J with FO PD(1+PI) with EV compared to PID, PD(1+PI), and FO PD(1+PI) are 75.64%, 59.18%, and 52.06%, respectively, for case 3.

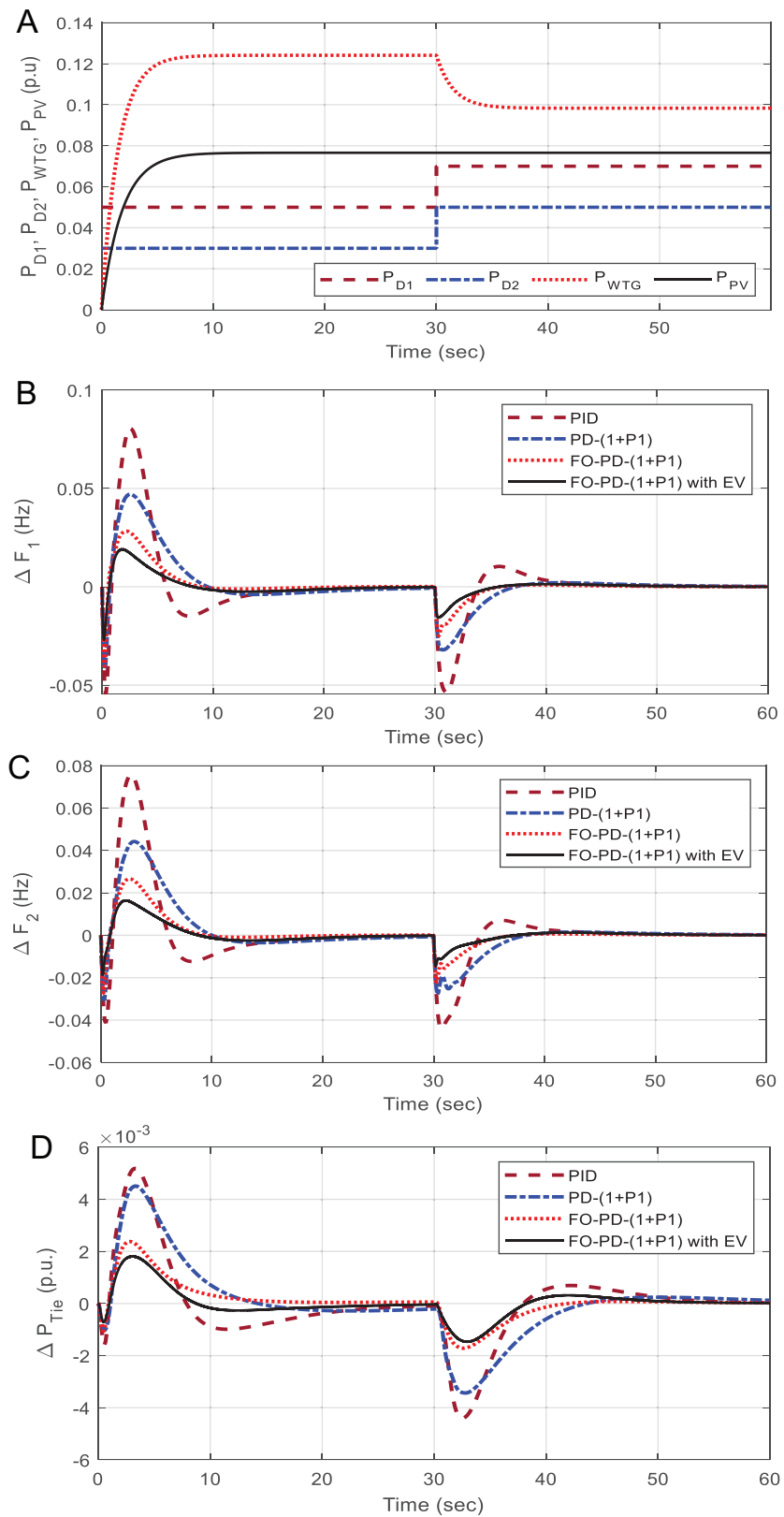


**Fig. 6.** (A–D) System responses of different disturbances, frequency deviation, and Tie line power deviation for case 2. (A)  $P_{D1}$ ,  $P_{D2}$ ,  $P_{WTG}$ ,  $P_{PV}$ , (B)  $\Delta F_1$ , (C)  $\Delta F_2$ , (D)  $\Delta P_{Tie}$

**TABLE V.** COMPARATIVE OF CONTROLLER'S PERFORMANCE INDEXES FOR CASE 2 USE OF HAOA-LUS TECHNIQUE

Controller/Method	Objective Function (J)	Integral Errors					MO <sub>s</sub>		MU <sub>s</sub> (-ve)	
		ISE	ITAE	ITSE	IAE	ISTAE	ΔF <sub>1</sub>	ΔF <sub>2</sub>	ΔF <sub>1</sub>	ΔF <sub>2</sub>
PID	4.5960	0.0393	15.5334	0.3749	1.0629	447.4062	0.0104	0.0071	0.0536	0.0439
PD-(1+PI)	2.6153	0.0187	12.706	0.1855	0.8189	375.3543	0.0021	0.0015	0.0321	0.0280
FO PD-(1+PI)	1.9874	0.0061	5.3449	0.0551	0.3927	155.5200	0.0010	0.0006	0.0249	0.0222
FO PD-(1+PI) with EV	0.9166	0.0027	5.0573	0.0255	0.3184	151.6492	0.0013	0.0012	0.0157	0.0147

EV, electric vehicle; FO, functional order; ISE, integral square error; PD-(1+PI), proportional derivative cascaded with one plus proportional integral controller.

#### D. Case 4

In real-world systems are likely to use parameters with some degree of imprecision, and they may change over time. This can have an effect on performance. Thus, investigating the system's performance when parameter changes are made is very essential. This requires a change of  $\pm 50\%$  in a step of 25% in the system parameter of gains and time constants of all components. Table VII collects the evaluation of description for the various scenarios as defined in the above analysis. The frequency response of area 1 for the above case with FO PD(1+PI) with EV is presented in Fig. 8. It is obvious from Table VII and Fig. 8 that hAOA-LUS tuned FO PD(1+PI) with EV method for frequency regulation is robust and works effectively in existence uncertainty of parameter.

#### E. Case 5

The primary characteristics of nonlinearities that exist in power systems must be taken into account in order to have a clear understanding of the AGC problem. The GRC and GBD are the two main nonlinearities that have a significant impact on the performance of the power system [23]. In view of the aforementioned, the analysis is further expanded to a more realistic power system by including the influence of GRC and GBD. A GRC of 3 %/min and GBD of 0.036 Hz are considered for the thermal system in the current study. For the hydro plant, GRC is comparatively considerably greater and a GRC of 4.5 %/s for rising generation and 6 %/s for reducing generation is assumed in the system. To investigate the effect of physical constraints, the tuning controller parameters which were found without considering nonlinearities are used for the power system with nonlinearities and all variations as given in case 5 are considered. The dynamic response with suggested hAOA-LUS optimized PID, PD(1+PI), FO PD(1+PI), and FO PD(1+PI) with EV are presented in Fig. 9 a-c. It can be seen from Fig. 9a-c that the system's performance reduces when nonlinearities are added in the system model. However, FO PD(1+PI) with EV gives superior performances compared to PID, PD(1+PI), and FO PD-(1+PI) controllers. The relative performances of transient features of different integral errors, maximum overshoots, maximum undershoots of  $\Delta F_1$ ,  $\Delta F_2$ ,  $\Delta P_{Tie}$  of the suggested system for case 5 are shown in Table VIII. It is clear from this Table VIII that the objective function values J, integral errors, MOs, and MUs owing to FO PD(1+PI) with EV are determined to be the least compare to other methods. The percentage improvement of the objective function J value with the suggested FO PD(1+PI) with EV compared to PID, PD(1+PI), and FO PD(1+PI) are 90.63%, 83.5%, and 77.39%, respectively, for case 5.

#### F. Case 6: Comparison With Recent Frequency Control Methods

For comparison with recent frequency control approaches, a two-area test system is considered [34]. For a fair comparison, the same

objective function and individual controllers in each area as given in [34] is are considered. The optimized results are given in Table IX. It is clear from the table that a lower ISE value is attained with the AOA-LUS: PID approach compared to Jaya: PID and MGOA: PID. The ISE value is further reduced when the AOA-LUS: FOPD(1+PI) controller is used. The frequency deviation response of area 1 is shown in Fig. 10, which demonstrates the superior performance of AOA-LUS: FOPD(1+PI) compared to recently proposed frequency control approaches.

#### G. Case 7: Comparison With OPAL-RT Result

The MMG system is simulated using hardware-in-the-loop (HIL) techniques to assess controller performance with final best values. To determine the suggested technique's practicable real-time implementable capacity, HIL real-time simulation is conducted. The HIL experimental setup utilized in this investigation is depicted in Fig. 11a. It consists of three components: 1) a host PC where the MATLAB/Simulink-based code to be performed on the OPAL-RT is built; 2) OPAL-RT as a real-time simulator; and 3) a router to link all of the setup devices in the same sub-network. The Intel Xeon E5, a 4. core, 3.0 GHz CPU with 8 GB of RAM, is the brains behind the OPAL-RT real-time simulator model, OP5700. The operating system for real-time simulator is Redhat v2.6.29.6-opalrt-6.2.1. Fig. 11b illustrates the HIL setup compilation process. Further information regarding HIL simulation based on OPAL-RT is available in [35-38].

The off-line simulations exclude the adjournments and errors caused by uncertainty that are present by nature but are included in the OPAL-RT. The initialization of the Simulink model via OPAL-RT lab, transformation of the model into an RT application, running of the same using multiple cores, and data gathering using the graphical user interface are the steps of real-time validations. The OPAL-RT setup is shown in Fig. 11a. The RT lab results versus Matlab results are shown in Fig. 11. In this situation all variants as indicated in case 3 are evaluated. It is clear from close observation that the responses are quite similar to each other justifying the feasibility of the proposed work.

## 5. CONCLUSION

In this article, a hybrid AOA and LUS approach is suggested for finding FO PD(1+PI) controller parameters for frequency control power systems with solar, wind, and EV sources. The proposed hAOA-LUS technique is applied to design PID controllers initially, and results are compared with GA, PSO, and AOA approaches. It is observed that the % decrease in J value using the hAOA-LUS approach compared to GA, PSO, and AOA are 78.05%, 72.01%, and 56.75%, respectively. In the next step, PD(1+PI), FO PD(1+PI), and FO PD(1+PI) with EV

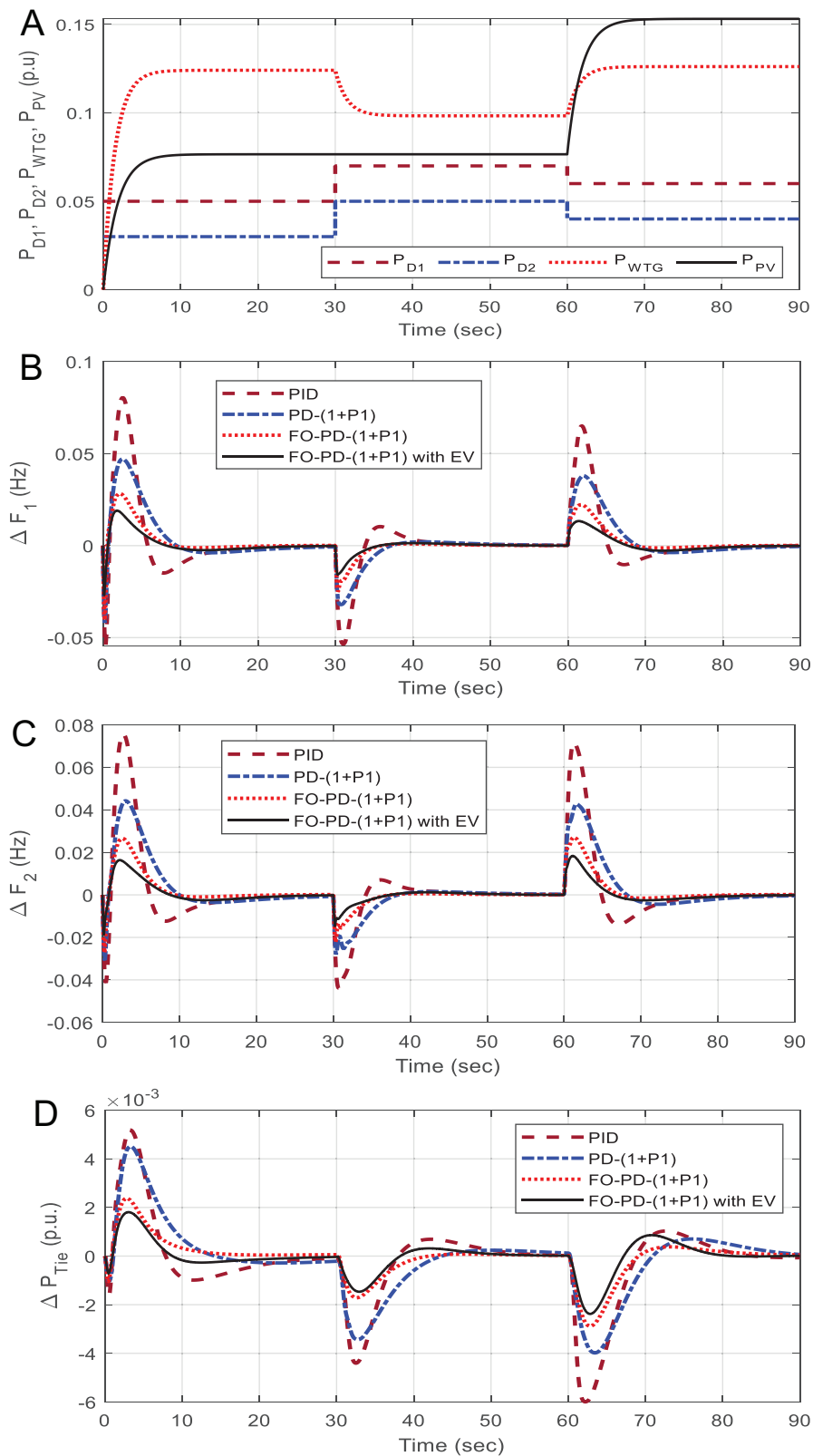


**Fig. 7.** (A–D) System responses of different disturbances, frequency deviation, and tie line power deviation for case 3. (A)  $P_{D1}$ ,  $P_{D2}$ ,  $P_{WTG}$ ,  $P_{PV}$ , (B)  $\Delta F_1$ , (C)  $\Delta F_2$ , (D)  $\Delta P_{Tie}$ .

**TABLE VI.** PERFORMANCE INDEX ASSESSMENT USED HAOA-LUS TUNING CONTROLLERS' PARAMETERS OF CASE 3

Controller/Method	Objective Function (J)	Integral Errors					MO <sub>s</sub>		MU <sub>s</sub> (-ve)	
		ISE	ITAE	ITSE	IAE	ISTAE	ΔF <sub>1</sub>	ΔF <sub>2</sub>	ΔF <sub>1</sub>	ΔF <sub>2</sub>
PID	7.8548	0.0607	52.9953	1.7084	1.6436	2.8754x10 <sup>3</sup>	0.0651	0.0716	0.0103	0.0139
PD-(1+PI)	4.6879	0.0296	44.2366	0.8705	1.2976	2.4699x10 <sup>3</sup>	0.0380	0.0427	0.0038	0.0044
FO PD-(1+PI)	3.9915	0.0095	19.9428	0.2688	0.6209	1.0936x10 <sup>3</sup>	0.0222	0.0271	0.0012	0.0015
FO PD-(1+PI) with EV	1.9133	0.0041	17.4699	0.1173	0.5054	0.9828x10 <sup>3</sup>	0.0133	0.0183	0.0027	0.0025

FO, functional order; ISE, integral square error; PD-(1+PI), proportional derivative cascaded with one plus proportional integral controller.

are taken for the analysis of the system. It is noted that, for similar step load perturbations in each area, the % decrease in J value with FO PD(1+PI) with EV compared to PD(1+PI) and FO PD(1+PI) are 77.5%, 61.36%, and 46.94%, respectively. When disturbances in load wind and solar power are considered (case 3) the % reduction in J value with FO PD-(1+PI) with EV compared to PID, PD(1+PI), and FO PD(1+PI) are 75.64%, 59.18%, and 52.06%, respectively. It is also

found that the suggested hAOA-LUS optimized FO PD(1+PI) with EV scheme for frequency regulation is resilient and works effectively in the presence of parameter uncertainty in the range ±50%. It is also noticed that the suggested technique can manage nonlinearities like GDB and GRC. When nonlinearities are included in the system model the percentage improvement in J value with the suggested FO PD(1+PI) with EV compared to PID, PD(1+PI), and FO PD(1+PI)

**TABLE VII.** COMPARATIVE PERFORMANCE INDEX VALUE FOR CONTROLLERS IN CASE 4 USED HAOA-LUS TECHNIQUE

Controller/ Method	Objective Function (J)	Integral Errors					% Change in J
		ISE	ITAE	ITSE	IAE	ISTAE	
+50%							
PID	8.2055	0.0609	52.6410	1.6689	1.6368	2.8728e+03	4.46
PD-(1+PI)	5.4004	0.0327	49.6725	0.9620	1.4526	2.7732e+03	15.19
FO PD-(1+PI)	4.2400	0.0109	22.8683	0.3086	0.7046	1.2604e+03	6.22
FO PD-(1+PI) with EV	2.2150	0.0045	19.1092	0.1299	0.5436	1.0857e+03	15.76
+25%							
PID	8.2782	0.0629	54.5966	1.7501	1.6885	2.9744e+03	5.39
PD-(1+PI)	5.1908	0.0324	48.4632	0.9525	1.4130	2.7115e+03	10.72
FO PD-(1+PI)	4.1750	0.0106	21.9987	0.3004	0.6791	1.2102e+03	4.59
FO PD-(1+PI) with EV	2.1824	0.0045	18.8348	0.1279	0.5383	1.0661e+03	14.06
-25%							
PID	6.5668	0.0506	46.3152	1.4365	1.4493	2.5008e+03	-16.39
PD-(1+PI)	3.8027	0.0236	36.6942	0.6937	1.0911	2.0380e+03	-18.88
FO PD-(1+PI)	3.2084	0.0075	16.6093	0.2081	0.5239	908.0235	-19.61
FO PD-(1+PI) with EV	1.6435	0.0034	14.9025	0.0956	0.4381	832.9663	-14.10
-50%							
PID	4.3040	0.0315	34.2134	0.9023	1.0798	1.8463e+03	-45.21
PD-(1+PI)	2.6151	0.0152	28.9928	0.4550	0.8496	1.6137e+03	-44.21
FO PD-(1+PI)	2.2556	0.0045	12.4234	0.1248	0.3964	676.4775	-43.48
FO PD-(1+PI) with EV	1.0409	0.0022	11.1432	0.0623	0.3323	619.7820	-45.59

EV, electric vehicle; FO, functional order; ISE, integral square error; PD(1+PI), proportional derivative cascaded with one plus proportional integral controller.

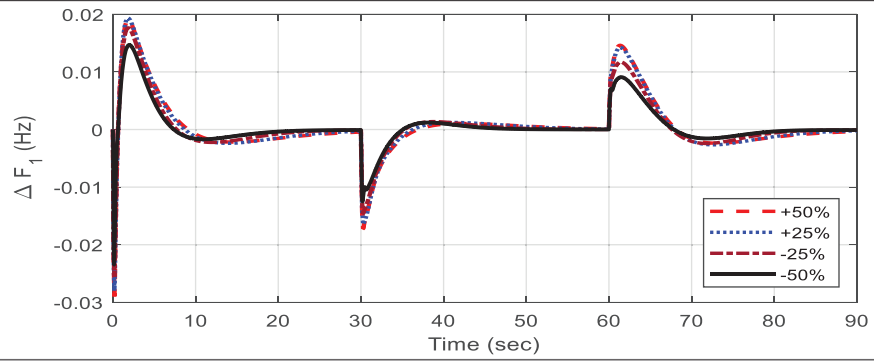


**Fig. 8.** Frequency deviation of area1  $\Delta F_1$  response with FO PD(PI+1) with EV for case 4.

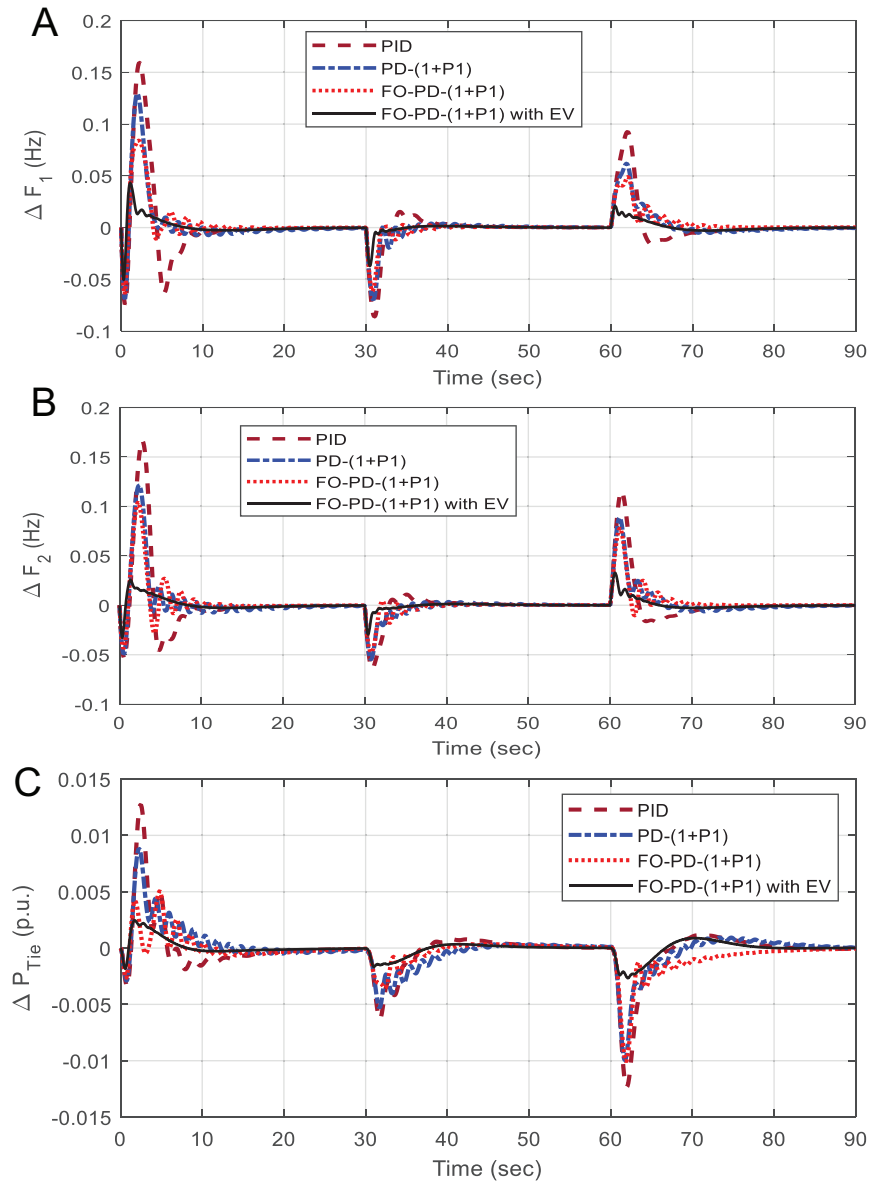


**Fig. 9.** (A–C) System response for case 5. (A)  $\Delta F_1$ , (B)  $\Delta F_2$ , (C)  $\Delta P_{Tie}$ .

**TABLE VIII.** COMPARATIVE PERFORMANCE INDEX VALUE FOR CONTROLLERS IN CASE 5 USED HAOA-LUS TECHNIQUE

Controller/ Method	Objective function (J)	Integral errors					MO <sub>s</sub>		MU <sub>s</sub> (-ve)	
		ISE	ITAE	ITSE	IAE	ISTA	ΔF <sub>1</sub>	ΔF <sub>2</sub>	ΔF <sub>1</sub>	ΔF <sub>2</sub>
PID	16.0372	0.14078	58.743	2.856	2.102	313.855	0.159	0.166	0.0861	0.063
PD-(1+PI)	9.1036	0.06965	44.361	1.389	1.447	245.147	0.129	0.121	0.069	0.054
FO PD-(1+PI)	6.6441	0.04831	33.582	1.025	1.151	183.441	0.084	0.104	0.064	0.047
FO PD-(1+PI) with EV	1.502	0.0071	17.631	0.1574	0.556	98.401	0.043	0.032	0.051	0.032

FO, functional order; ISE, integral square error; PD-(1+PI), proportional derivative cascaded with one plus proportional integral controller.

**TABLE IX.** OPTIMIZED CONTROLLER PARAMETERS OF THE PROPOSED TWO-AREA TEST SYSTEM [34]

Techniques/Controller	Jaya: PID	MGOA: PID	AOA-LUS: PID	AOA-LUS: FOPD-(1+PI)
K <sub>p1</sub>	1.9504	2.954	2.9830	2.9830
K <sub>i1</sub>	1.9210	2.733	2.9815	2.9815
K <sub>d1</sub>	0.8168	1.892	2.9815	2.4832
K <sub>p2</sub>	1.9504	2.844	2.9830	2.9830
K <sub>i2</sub>	1.9210	2.935	2.9815	2.9815
K <sub>d2</sub>	0.8168	1.887	2.9815	2.9815
K <sub>pp1</sub>				2.9830
K <sub>pp2</sub>				2.9815
λ <sub>1</sub>				1.1617
λ <sub>2</sub>				1.4840
μ <sub>1</sub>				1.0708
μ <sub>2</sub>				1.2957
ISE	6.0215e-04	2.7551e-04	2.3918e-04	0.21328e-04

AOA, Arithmetic Optimization Algorithm; FO, functional order; ISE, integral square error; LUS, Local Unimodal Sampling; PD-(1+PI), proportional derivative cascaded with one plus proportional integral controller.

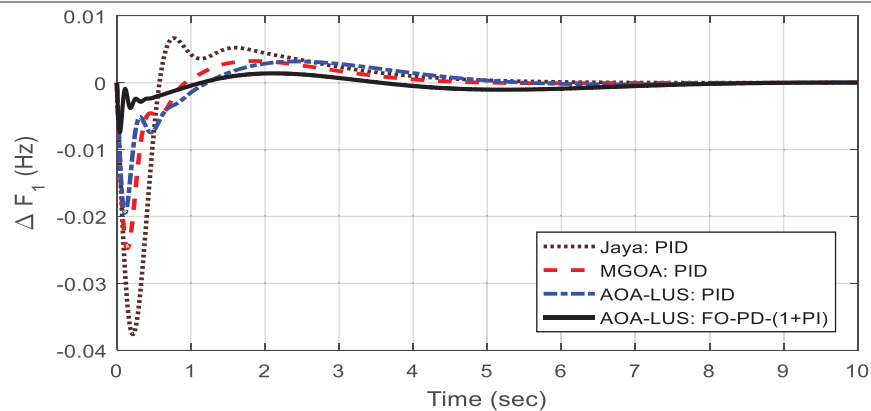


**Fig. 10.** Frequency deviation response of area 1.

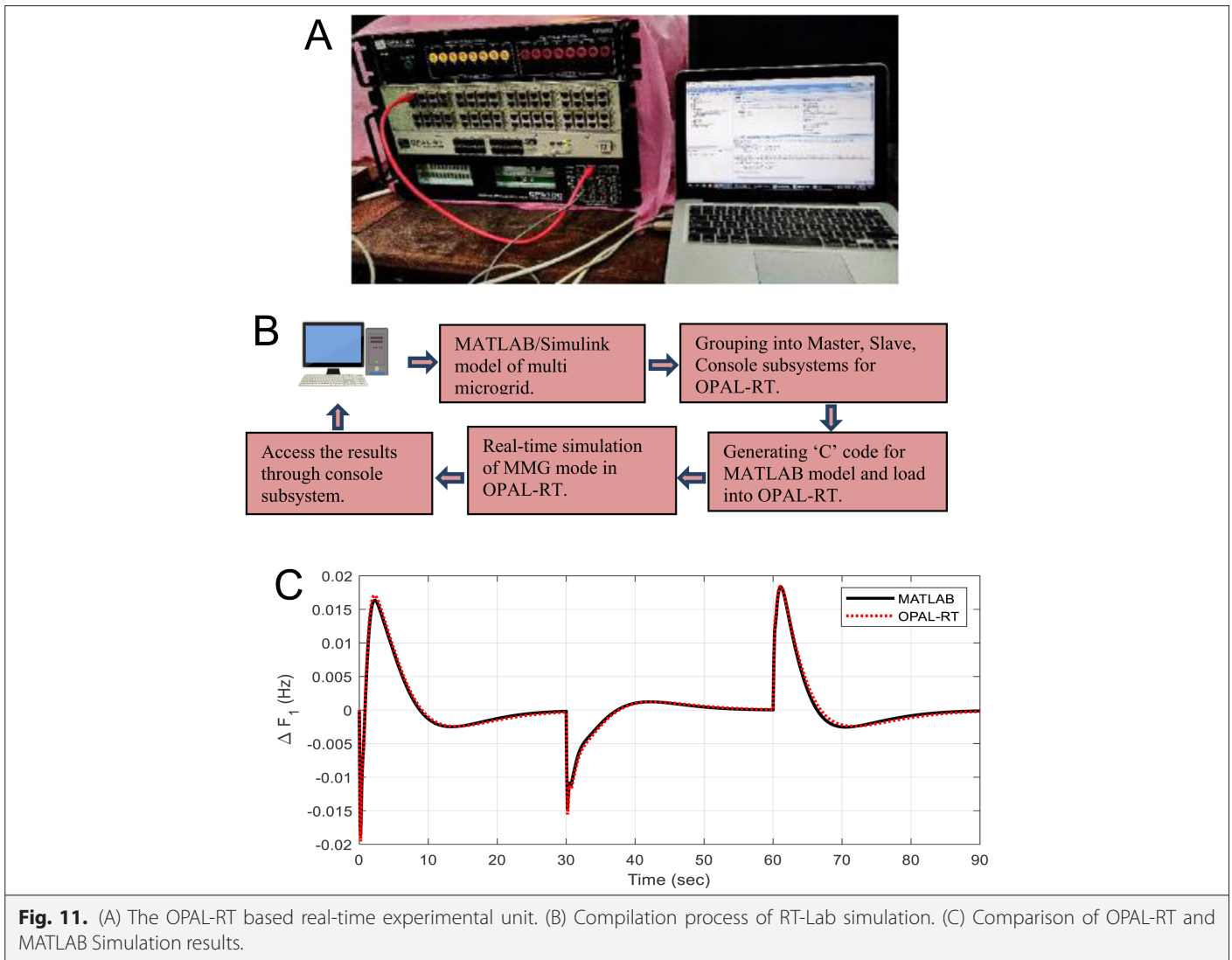


**Fig. 11.** (A) The OPAL-RT based real-time experimental unit. (B) Compilation process of RT-Lab simulation. (C) Comparison of OPAL-RT and MATLAB Simulation results.

are 90.63%, 83.5%, and 77.39%, respectively. To verify the scheme's viability, MATLAB simulation results are compared to OPAL results. It is also found that MATLAB in Simulink results are extremely similar to OPAL-RT results.

**Peer-review:** Externally peer-reviewed.

**Author Contributions:** Concept – S.K.M., A.K.B.; Design – S.K.M.; Supervision – S.K.M., P.M.D.; Resources – A.K.B., S.K.M.; Materials – P.M.D., A.K.B.; Data Collection and/or Processing – A.K.B., S.K.M.; Analysis and/or Interpretation – S.K.M., A.K.B.; Literature Search – A.K.B., P.M.D.; Writing – S.K.M., A.K.B.; Critical Review – S.K.M., A.K.B.

**Declaration of Interests:** The authors have no conflict of interest to declare.

**Funding:** The authors declared that this study has received no financial support.

## REFERENCES

1. P. Kundur, *Power System Stability and Control*. New Delhi: Tata McGraw Hill, 2009.
2. O. L. Elgerd, *Electric Energy Systems Theory – An Introduction*. New Delhi: Tata McGraw Hill, 2000.
3. C. Fosha, and O. I. Elgerd, "The megawatt-frequency control problem: A new approach via optimal control theory," *IEEE Trans. Power Apparatus Syst.*, vol. 4, no. 4, pp. 563–577, 1970. [\[CrossRef\]](#)
4. L. C. Saikia, J. Nanda, and S. Mishra, "Performance comparison of several classical controllers in AGC for multi-area interconnected thermal system," *Int. J. Electr. Power Energy Syst.*, vol. 33, no. 3, pp. 394–401, 2011. [\[CrossRef\]](#)
5. P. Dash, L. C. Saikia, and N. Sinha, *Flower Pollination Algorithm Optimized PI-PD Cascade Controller in Automatic Generation Control Multi-area Power System*, *Electrical Power and Energy Systems*, Vol. 82, pp. 19–28, 2016.
6. P. Dash, L. C. Saikia, and N. Sinha, "Automatic generation control of a multi area thermal system using Bat algorithm optimized PD-PID cascade controller," *Electr. Power Energy Syst.*, vol. 68, pp. 364–372, 2015. [\[CrossRef\]](#)
7. R. K. Sahu, S. Panda, S., and U. K. Rout, "DE optimized parallel 2-dof PID controller for load frequency control of power system with governor dead-band nonlinearity," *Electr. Power Energy Syst.*, vol. 49, pp. 19–33, 2013.
8. P. C. Nayak, U. C. Prusty, R. C. Prusty and A. Barisal, "Application of SOS in Fuzzy Based PID Controller for AGC of Multi-area Power System," *IEEE conference on Technologies for Smart – City Energy Security and Power*, Vol. 1, 2018, pp.1–6.
9. R. K. Sahu, S. Panda, and G. T. C. Sekhar, "A novel hybrid PSO-PS optimized fuzzy PI controller for AGC in multi area interconnected power systems," *Electr. Power Energy Syst.*, vol. 64, pp. 880–893, 2015.
10. I. Podlubny, "Fractional-order systems and PI/sup /spl lambda/ /D/ sup /spl mu/ -controllers," *IEEE Trans. Autom. Control*, vol. 44, No. 1, January, 208–214, 1999. [\[CrossRef\]](#)

11. I. Paducel, C. O. Safirescu, and E. Dulf, "Fractional Order Controller Des. Wind Turbine," *Applied Science*, vol. 12, p. 8400, 2022.
12. P. M. Dash, A. K. Baliarsingh, and S. K. Mohapatra, "Hybrid African vulture optimization algorithm and pattern search tuned fractional order PID controller for AGC of electric vehicles integrated power systems," *Int. J. Electr. Eng. Inform.*, vol.15, no.2, pp. 259–276, 2023. [\[CrossRef\]](#)
13. P. C. Sahu, R. C. Prusty, and S. Panda, "Optimal design of a robust FO-Multistage controller for the frequency awareness of an islanded AC microgrid under i-SCA algorithm," *Int. J. Ambient Energy*, vol. 43, no. 1, pp. 2681–2693, 2022. [\[CrossRef\]](#)
14. P. C. Sahu, R. C. Prusty, and S. Panda, "Improved-GWO designed FO based type-II fuzzy controller for frequency awareness of an AC microgrid under plug in electric vehicle," *J. Ambient Intell. Hum. Comput.*, vol. 12, no. 2, 1879–1896, 2021. [\[CrossRef\]](#)
15. W. Kempton, and J. Tomic, "Vehicle-to-grid power implementation: From stabilizing the grid to supporting large-scale renewable energy," *J. Power Sources*, vol. 144, no. 1, pp. 280–294, 2005. [\[CrossRef\]](#)
16. H. Liu, Z.Hu, Y. Song, and J. Lin, "Decentralized vehicle-to-grid control for primary frequency regulation considering charging demands" *IEEE Trans. Power Syst.*, vol. 28, no. 3, pp. 3480–3489, 2013. [\[CrossRef\]](#)
17. S. Padhy, and S. Panda, "Application of a simplified Grey Wolf optimization technique for adaptive fuzzy PID controller design for frequency regulation of a distributed power generation system," *Prot. Control Mod. Power Syst.*, vol. 6, no. 1, pp. 1–16, 2021.
18. S. K. Bhatta, S. Mohapatra, P. C. Sahu, S. C. Swain, and S. Panda, "Load frequency control of a diverse energy source integrated hybrid power system with a novel hybridized harmony search-random search algorithm designed Fuzzy-3D controller," *Energy Sources A*, pp. 1–22, 2021.
19. P. C. Sahu, R. C. Prusty, and S. Panda, "Active power management in wind/solar farm integrated hybrid power system with AI based 3DOF-FOPID approach," *Energy Sources A*, pp. 1–21, 2021. [\[CrossRef\]](#)
20. P. C. Pradhan, R. K. Sahu, and S. Panda, "Comparative performance analysis of hybrid differential evolution and pattern search technique for frequency control of the electric power system," *J. Electr. Syst. Inf. Technol.*, vol. 8, pp. 1–21, 2021.
21. D. Mohanty, R. K. Sahu, P. C. Pradhan, and S. Panda, "Design and analysis of the 2DOF-PIDN-FOID controller for frequency regulation of the electric power systems," *Int. J. Ambient Energy*, pp. 1–14, 2021.
22. P. C. Sahu, R. C. Prusty, and S. Panda, "Grasshopper optimization algorithm optimized multistage controller for automatic generation control of a power system with FACTS devices," *Prot. Control Mod. Power Syst.*, vol. 6, pp. 1–15, 2021.
23. P. C. Nayak, B. P. Nayak, R. C. Prusty, and S. Panda, "Sunflower optimization based fractional order fuzzy PID controller for frequency regulation of solar-wind integrated power system with hydrogen aqua equalizer-fuel cell unit," *Energy Sources A*, pp. 1–19, 2021.
24. S. Mishra, R. C. Prusty, and S. Panda, "Performance analysis of modified sine cosine optimized multistage FOPD-PI controller for load frequency control of an islanded microgrid system," *Int. J. Numer. Modell. Electron. Netw. Devices Fields*, vol. 34, no. 6, 2021. [\[CrossRef\]](#)
25. P. C. Nayak, A. Sahoo, R. Balabantaray, and R. C. Prusty, "Comparative study of SOS & PSO for fuzzy based PID controller in AGC in an integrated power system," IEEE conference on Technologies for Smart – City Energy Security and Power, Vol. 1, pp. 1–6. [\[CrossRef\]](#)
26. R. K. Khadanga, A. Kumar, and S. Panda, "Application of interval Type-2 fuzzy PID controller for frequency regulation of AC islanded microgrid using modified equilibrium optimization algorithm," *Arab. J. Sci. Eng.*, vol. 46, no. 10, pp. 9831–9847, 2021. [\[CrossRef\]](#)
27. P. R. Sahu, "P. K. Hota and S. Panda, Power System Stability Enhancement by Fractional Order Multi-input SSSC Based Controller Employing Whale Optimizing Algorithm," *Electr. Syst. Inform Technol.*, vol. 5, no. 3, pp. 326–336, 2018.
28. S. Padhy, S. Panda, and S. Mahapatra, "A modified GWO technique-based cascade PI-PD controller for AGC of power systems in presence of plug in Electric vehicles," *Eng. Sci. Technol.*, vol. 20, no. 2, pp. 427–442, 2017. [\[CrossRef\]](#)
29. P. C. Sahu, R. C. Prusty, and S. Panda, "A gray wolf optimized FPD plus (1+PI) multistage controller for AGC of multisource non-linear power system," *World J. Eng.*, vol. 16, no. 1, 1–13, 2019. [\[CrossRef\]](#)
30. L. Abualigaha, A. Diabat, S. Mirjalili, M. F. Elaziz, and A. H. Gandomi, "The arithmetic optimization algorithm," *Comput. Methods Appl. Mech. Eng.*, vol. 376, p. 113609, 2021.
31. M. E. H. Pedersen, *Tuning & Simplifying Heuristical Optimization* (PhD Thesis). United Kingdom: School of Engineering Sciences, University of Southampton, 2010.
32. I. Pan, and S. Das, "Kriging based surrogate modeling for fractional order control of microgrids," *IEEE Trans. Smart Grid*, vol. 6, no. 1, pp. 36–44, 2015. [\[CrossRef\]](#)
33. R. K. Khadanga, A. Kumar, and S. Panda, "Frequency control in hybrid distributed power systems via type-2 fuzzy PID controller," *IET Renew. Power Gener.*, vol. 15, no. 8, pp. 1706–1723, 2021. [\[CrossRef\]](#)
34. S. G. Orimi, and A. G., "Marzbali, Load Frequency Control of Multi-area Multi-source System with Nonlinear Structures Using Modified Grasshopper Optimization Algorithm," *Appl. Soft Comput.*, vol. 137, p. 11013, 2023.
35. M. H. Khooban, T. Dragicevic, F. Blaabjerg, and M. Delimar, "Shipboard microgrids: A novel approach to load frequency control," *IEEE Trans. Sustain. Energy*, vol. 9, no. 2, pp. 843–852, 2017. [\[CrossRef\]](#)
36. M. H. Khooban, T. Niknam, F. Blaabjerg, and T. Dragičević, "A new load frequency control strategy for micro-grids with considering electrical vehicles," *Electr. Power Syst. Res.*, vol. 143, pp. 585–598, 2017. [\[CrossRef\]](#)
37. M. H. Khooban, T. Niknam, M. Shasadeghi, T. Dragicevic, and F. Blaabjerg, "Load frequency control in microgrids based on a stochastic noninteger controller," *IEEE Trans. Sustain. Energy*, vol. 9, no. 2, pp. 853–861, 2017. [\[CrossRef\]](#)
38. M. Gheisarnejad, and M. H. Khooban, "Secondary load frequency control for multi-microgrids: HiL real-time simulation," *Soft Comput.*, pp. 1–4, 2018.



Dr. Asini Kumar Baliarsingh received B.E degree in Electrical Engineering from Utkal University in 1998, M.Tech degree in 2004 from NIT, Jamesdpur, India, He received the Ph.D degree in the year 2012. He is currently working in Electrical Engineering Department in Government College of Engineering, Kalahandi, Odisha, India, He has published more than 40 paper in International Journal and Conferences. He has more than 22-year experience in teaching and research experience in the field of Electrical Engineering. He is member of ISTE, India. His research interest are in FACTS Controller, AI techniques, power system stability problem etc.



Dr. Sangram Keshori Mohapatra received BE degree in Electrical Engineering in the year 1999, M.Tech degree in the year of 2008 in the specialization of Power Electronics and Drives and Ph.D degree in the year of 2014 in the specialization of power system Engineering. He has acquired more than 22 years of experience in the field of Academics and Research pertaining to Electrical Engineering. Presently, he is working as an Associate Professor in Electrical Engineering, Government College of Engineering, Keonjhar a constituent college of BPUT, Odisha. He has published about 60 papers in international journal and conferences. He has guided 25 M.Tech research scholars. He is currently guiding 4 Ph.D Research scholars. He is the Life member of Indian Society for Technical Education (ISTE), India and Fellow of The Intuitions of Engineers (IEI) and member of IEEE and reviewer of various repute journals. His research interest is in the area of flexible AC transmission systems (FACTS), modeling of machines, power electronics, power systems and FACTS, controller design, power system stability, optimization techniques and automatic generation and control.



Mr. Pabitra Mohan Dash Graduated in Electrical Engineering in 1993, M.Tech Degree in Electrical Engineering in 2008 and Presently he is working as Associate Professor in Electrical Engineering, Bhubaneswar Engineering College, Bhubaneswar, Odisha and Research scholar under BPUT, Odisha. His research interests are the field of electrical power system and control, optimization techniques, flexible AC transmission controller and load frequency control.